Biosensors and Bioelectronics 143 (2019) 111623

Contents lists available at ScienceDirect

Biosensors and Bioelectronics

journal homepage: www.elsevier.com/locate/bios

Vertical capacitance aptasensors for real-time monitoring of bacterial growth and antibiotic susceptibility in blood

Jun Ho Song[a], Sun-Mi Lee[b], In Ho Park[c,d], Dongeun Yong[e], Kyo-Seok Lee[a], Jeon-Soo Shin[b,c,d,**], Kyung-Hwa Yoo[a,b,*]

[a] Department of Physics, Yonsei University, Seoul, 03722, Republic of Korea
[b] Nanomedical Graduate Program, Yonsei University, Seoul, 03722, Republic of Korea
[c] Department of Microbiology, Yonsei University College of Medicine, Seoul, 03722, Republic of Korea
[d] Severance Biomedical Science Institute, Institute for Immunology and Immunological Diseases, Yonsei University College of Medicine, Seoul, 03722, Republic of Korea
[e] Department of Laboratory Medicine and Research Institute of Bacterial Resistance, Yonsei University College of Medicine, Seoul, 03722, Republic of Korea

ARTICLE INFO

Keywords:
Bacterial growth
Biofilm
Antibiotic susceptibility
Blood
Vertical aptasensor

ABSTRACT

For the treatment of bacteremia, early diagnosis and rapid antibiotic susceptibility tests (ASTs) are necessary because survival chances decrease significantly if the proper antibiotic administration is delayed. However, conventional methods require several days from blood collection to AST as it requires three overnight cultures, including blood culture, subculture, and AST culture. Herein, we report a more rapid method of sensing bacterial growth and AST in blood based on a vertical capacitance sensor functionalized with aptamers. Owing to their vertical structure, the influence of blood cells sunk by gravity on capacitance measurements were minimized. Thus, bacterial growth in blood at 10^0–10^3 CFU/mL was monitored in real-time by measuring changes in capacitance at $f = 10$ kHz. Moreover, real-time capacitance measurements at $f = 0.5$ kHz provided information on biofilm formation induced during blood cultures. Bacterial growth and biofilm formation are inhibited above the minimal inhibitory concentration of antibiotics; therefore, we also demonstrated that vertical capacitance aptasensors could be applied to rapid AST from positive blood cultures without a need for the subculture process.

1. Introduction

Bacteremia is a serious medical condition characterized by high morbidity and mortality. It occurs when bacteria enter the bloodstream from infections in an organ or a wound, indwelling urethral catheters, or an implanted device, and multiply at a rate that exceeds removal by phagocytosis. Mortality attributed to bacteremia ranges from 20 to 50% (Caballero-Granado et al., 2001; Yilmaz et al., 2016; van Hal et al., 2012). Survival decreases drastically if the appropriate treatment is delayed; survival rate is reduced by 7.6% in the first hour and every hour thereafter (Kumar et al., 2009). However, if a patient receives effective antibiotic therapy within the first hour of diagnosis, chances of survival are close to 80%.

Considerable effort and attention has been directed toward providing rapid antibiotic susceptibility tests (AST) for directed therapy. However, conventional methods require > 3 d for AST results, because three overnight culture steps—blood culture, subculture, and AST culture—are required (Jorgensen and Ferraro, 2009; Leekha et al., 2011; Pulido et al., 2013). For blood culture, an optimal volume of blood is inoculated into bottles containing culture media, which are designed to accommodate the recommended blood-to-culture media ratio (1:5 to 1:10), and then incubated for up to 5 d. Blood culture positivity is generally detected by measuring the CO_2 produced when the microorganisms metabolize the substrates present in the bottle. The change in CO_2 levels is detected by measuring fluorescent signals, color changes, or redox variations in continuous-monitoring blood-culture systems (Pohlman et al., 1995; Lancaster et al., 2015; Chang et al., 2015; Almuhayawi et al., 2015).

Upon detection of blood culture positivity, a subculture from positive blood culture medium to fresh medium is performed for species identification and AST. In positive blood culture bottles, bacteria are mixed with a large number of blood cells; thus, the media cannot be used directly for conventional AST methods, such as broth dilution and disk diffusion methods (Balouiri et al., 2016; Luna et al., 2007). Molecular detection of resistance determinants, e.g., via polymerase chain reactions, provides fast identification of strains carrying specific

* Corresponding author. Department of Physics, Yonsei University, Seoul, 03722, Republic of Korea.
** Corresponding author. Nanomedical Graduate Program, Yonsei University, Seoul, 03722, Republic of Korea.
E-mail addresses: jsshin6203@yuhs.ac (J.-S. Shin), khyoo@yonsei.ac.kr (K.-H. Yoo).

https://doi.org/10.1016/j.bios.2019.111623
Received 5 June 2019; Received in revised form 20 August 2019; Accepted 21 August 2019
Available online 22 August 2019
0956-5663/

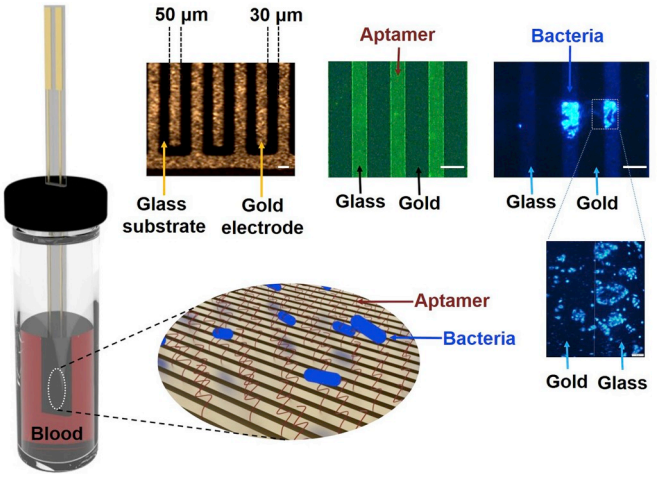

Fig. 1. Scheme of vertical capacitance aptasensor. Interdigitated Au electrodes with a width of 50 μm and a spacing of 30 μm were patterned on a glass substrate, and bacteria-aptamers were immobilized on the sensor surface between the electrodes. To minimize the influence of blood cells on the electrical properties, the fabricated sensor was vertically inserted into the lid of a 2-mL bottle. The first inset shows an optical image of the fabricated sensor, and the second inset shows a fluorescence image acquired from the sensor surface after the immobilization of the fluorescence-modified aptamers. The third inset presents a fluorescence image of the sensor stained with DAPI after the blood culture. The bright blue color indicates the *E. coli* bound on the sensor surface via the aptamers. Scale bars, 50 μm. (For interpretation of the references to color in this figure legend, the reader is referred to the Web version of this article.)

antibiotic resistance genes (~2 h) (Oliveira and de Lencastre, 2002; Baym et al., 2016; Bradley et al., 2015). However, these methods may fail in cases where the newly acquired antibiotic resistance is independent of the target gene expression. Recently, in order to reduce the time needed to obtain conventional AST results (1.5–2 d), rapid image-based technologies for AST using positive blood cultures, which combine gel electrofiltration and fluorescence *in situ* hybridization for bacterial identification, as well as automated microscopy for analyzing bacterial growth rates (Chantell, 2015; Brazelton de Cárdenas et al., 2017) have been developed. In addition to image-based methods, rapid ASTs using electrical measurements were investigated because of their label-free and rapid detection (Safavieh et al., 2017; Nazemi et al., 2017; Zhang et al., 2018; Jo et al., 2018; Webster et al., 2015). However, most electrical biosensors have electrodes on the bottom making them unsuitable for detecting bacterial growth in blood. In addition, non-specifically precipitated blood cells can interfere with the electrical signals.

Herein, we report a vertical-type aptamer-functionalized sensor (aptasensor) that is vertically connected to a measurement system (Fig. 1 and Fig. S1). When bacteria were cultured in blood culture media comprising blood (0.2 mL) and culture media (0.8 mL), we found that the capacitance changes measured at $f = 0.5$ and 10 kHz reflected the biofilm formation and bacterial growth, respectively, allowing their simultaneous monitoring. Bacteria seeded at 10^0–10^3 CFU/mL could be detected within 12 h by measuring the capacitance changes at $f = 0.5$ and 10 kHz, indicating that the vertical capacitance aptasensor can be an alternative tool to CO_2 detection for detecting bacteria in blood. Additionally, the susceptibility of bacterial growth and biofilm formation in the blood could be measured in the presence of antibiotics. These results demonstrate that the vertical capacitance aptasensor can be employed for rapid ASTs using positive blood cultures as well as for bacterial detection in blood.

2. Materials and method

2.1. Bacterial strains, growth condition, antibiotic solutions

Escherichia coli (*E. coli*) ATCC 25922, *Pseudomonas aeruginosa* (*P. aeruginosa*) ATCC 27853, and *Staphylococcus aureus* (*S. aureus*) ATCC 29213 strains were used in this study. Mutant strains, i.e., *Δpel* and *Δpel/Δpsl* of *P. aeruginosa* strain PAO1, were obtained from the laboratories of Yonsei University Severance Hospital. Antibiotics, gentamicin and amikacin were purchased from Sigma-Aldrich (St. Louis, MO, USA). For the blood culture media, whole sheep blood (Synergy Innovation co., Ltd., Korea) was mixed with bacterial culture media (Difco™ & BBL™) at a 1:4 vol ratio. To estimate the effects of the antibiotics, 10 mg/mL stock solutions of each antibiotic were prepared in ultra-pure water and diluted in a growth medium.

2.2. DNA aptamer

The sequence of each DNA aptamer specific to the bacteria was as follows: *E. coli*, 5'-GCA ATG GTA CGG TAC TTC CCC ATG AGT GTT GTG AAA TGT TGG GAC ACT AGG TGG CAT AGA GCC GCA AAA GTG CAC GCT ACT TTG CTA A-3' (Kim et al., 2014); *P. aeruginosa*, 5'-CCC CCG TTG CTT TCG CTT TTC CTT TCG CTT TTG TTC GTT TCG TCC CTG CTT CCT TTC TTG-$(CH_2)_3$'-SH-3' (Kim et al., 2017); and *S. aureus*, 5'-GCA ATG GTA CGG TAC TTC CTC GGC ACG TTC TCA GTA GCG CTC GCT GGT CAT CCC ACA GCT ACG TCA AAA GTG CAC GCT ACT TTG CTA A-3' (Lian et al., 2015). All aptamers were custom-synthesized by Genotech Inc. (Daejeon, Korea) and dissolved to a concentration of 10 μM in distilled water for further use.

2.3. Fabrication of vertical capacitance sensor and aptamer immobilization on the sensor surface

The vertical capacitance sensor (50 μm width and 30 μm gap, with a working area of 4 × 2.2 mm^2; Fig. S1a) was fabricated on a glass substrate. As shown in Fig. 1, interdigitated chromium/gold (5 nm/50 nm) electrodes were patterned by photolithography and lift-off techniques. For electrical measurements, the sensor was placed in a hole in the lid of a 2-mL vial and sealed using epoxy after the sensor surface was immobilized with bacteria-aptamers.

To immobilize the bacteria-aptamers, the sensor was treated with a piranha solution (H_2O_2: H_2SO_4 = 1:3) for 3 min to form OH groups on the glass substrate. Subsequently, the sensor was treated with 10% (3-aminopropyl) triethoxysilane in ethanol for 1 h at room temperature and in the dark, then washed with absolute ethanol followed by distilled water twice. Afterwards, the sensor was cured for 30 min at 100 °C. To form carboxylic groups, the sensor was treated with 0.1 M succinic anhydride in ethanol for 2 h at room temperature, then washed with absolute ethanol and distilled water several times. To activate the carboxylic groups, the sensor was treated with 0.2 mM *N*-3-dimethylaminopropyl and 0.2 mM N-hydroxysulfosuccinimide in a 1 M MES solution for no less than 4 h, and then washed with distilled water several times. Finally, the sensor was incubated in a solution of 10 μM amine-modified aptamers for 1 h and washed thoroughly with distilled water. To detect *E. coli*, *S. aureus*, and *P. aeruginosa*, mixtures of *E. coli* –, *S. aureus* –, and *P. aeruginosa* – aptamers were immobilized on the sensor surface. All chemicals used were purchased from Sigma-Aldrich (St. Louis, MO. USA).

2.4. Electrical measurements

For the bacteria culture, a 2-mL glass vial (iNexus. Inc., Seongnam, Korea) was autoclaved at 120 °C, and 1 mL of blood culture media (sheep blood: culture media = 1:4) containing 10^0, 10^1, 10^2, or 10^3 CFU/mL bacteria was added to the vial. The sensor was mounted on a connector system that could measure the capacitance, conductance,

and impedance of 16 sensors simultaneously (Fig. S1b). This connector system was placed inside an incubator maintained at 37 °C, and measurements were recorded using an LCR meter (Agilent 4294A, Santa Clara, CA, USA) with a peak-to-peak alternating current signal of 10 mV at frequencies ranging from 0.5 to 10 kHz. The sensors and LCR meter inside and outside the incubator, respectively, were connected via electrical connectors that were mounted on the side of the incubator. The capacitance, conductance, and impedance were measured simultaneously for 16 sensors using a data acquisition/switching unit (Agilent) that was connected to the LCR meter. Data were collected every 16.5 min from every sensor.

2.5. Antibiotic susceptibility tests

Two antibiotics, gentamicin and amikacin, were selected as the model antibiotics for the ASTs. For the AST experiments, different concentrations of antibiotic solution (0.1 mL) were added to an autoclaved vial containing blood culture media (0.8 mL) and allowed to incubate for 30 min. Next, 10^4 CFU/mL bacteria (0.1 mL) was inoculated to the vial to obtain an initial concentration of 10^3 CFU/mL. The sensor containing the bacteria and antibiotic solutions was placed inside the incubator, which was maintained at 37 °C, and real-time capacitance measurements were performed in the frequency range of 0.5–10 kHz.

2.6. Analysis of biofilm formation

To estimate the formation of the biofilm, the sensor was stained with a crystal violet solution (Sigma-Aldrich). First, the bacteria on the sensor surface were fixed with 4% paraformaldehyde for 5 min, then washed twice with distilled water for 2 min each. Then, the bacteria were stained with the crystal violet solution for 10 min at room temperature and washed with distilled water twice for 2 min each. The stained electrodes were gently dried using an air gun. Images of the biofilm stained with crystal violet were obtained using an optical and scanning electron microscope (JSM–6500F, JEOL, Tokyo, Japan). To quantify the area of the formed biofilm, the stained images were analyzed using the ImageJ software (NIH, Bethesda, MD, USA).

3. Results and discussion

3.1. Aptamer-functionalized vertical sensor

The vertical aptasensor is schematically illustrated in Fig. 1. Interdigitated gold electrodes were fabricated on a glass surface, which was then chemically functionalized with bacteria-aptamers. The fabricated aptasensor was inserted into the lid of a bottle (2 mL) containing 1 mL of blood culture media with a 1:4 blood to culture media ratio and then connected to a measurement system that could read 16 sensors simultaneously (Fig. S1). As shown in the insets of Fig. 1, the bacteria were bound on the sensor surface via aptamers during the blood culture and affected the electrical properties.

3.2. Frequency dependence of capacitance, conductance, and impedance

Prior to the inoculation of bacteria, we measured the frequency dependence of the capacitance, conductance, and impedance in bacteria-free culture media (media) and blood culture media (blood) with a blood-to-culture media ratio of 1:4 before and after the immobilization of the bacteria-aptamers on the sensor surface (Fig. 2a – c). Similar to results of previous studies, as the frequency increased, capacitance and impedance decreased, whereas conductance increased (Jo et al., 2018; Song et al., 2018). However, the bacteria-free blood had a higher capacitance and conductance, but lower impedance, than the bacteria-free media owing to a large number of blood cells. After the immobilization of the aptamers, the capacitance and conductance increased, particularly at low frequencies, for both the media and blood, while the impedance decreased. These results indicate that the impedance of the aptamers ($Z_{aptamer}$) was lower than that of the bacteria-free solution ($Z_{free\text{-}solution}$), resulting in a decrease in the total impedance given by $Z_{tot} = (1/Z_{free\text{-}solution} + 1/Z_{aptamer})^{-1}$, as shown in Fig. 2d. Here, the interface impedance ($Z_{interface}$) is assumed to be negligible.

Fig. 2e – g shows the frequency dependence of capacitance, conductance, and impedance, respectively, which were measured using the vertical aptasensor at 0 and 18 h after inoculating 10^3 CFU/mL *E. coli* into the media or blood. For the media culture, the capacitance and conductance increased and the impedance decreased at all frequencies, implying that the impedance of the bacteria bound on the sensor surface via aptamers ($Z_{bacteria}$) was smaller than that of $Z_{aptamer}$ (Fig. 2h). However, for the blood culture, capacitance decreased at low frequencies and increased at high frequencies, resulting in a crossover at 2.5 kHz (inset of Fig. 2e). However, in contrast to the media culture, the conductance decreased and the impedance increased at all frequencies (insets of Fig. 2f and g).

To investigate the origin of these different behaviors observed for the media and blood cultures, we examined the sensor surfaces using scanning electron microscopy (SEM) and crystal violet staining after the electrical measurements. The SEM images indicate that *E. coli* formed larger clusters in the blood than in the media (Fig. 2i). In addition, positive (violet) staining was clearly observed on the sensor surface for the blood culture, but not for the media culture (Fig. 2j). These findings revealed that the bacteria biofilm did not form within 18 h for the media culture, but did for the blood culture. The biofilm is known to have high impedance values, which decrease rapidly with increasing frequency (Liu et al., 2018). Therefore, the increase in impedance observed at low frequencies for the blood culture was possibly due to the formation of the biofilm in the blood.

3.3. Influence of biofilm on electrical properties

Fig. 3a – c shows real-time capacitance, conductance, and impedance, respectively, which were measured at $f = 0.5$ and 10 kHz when *E. coli,* at 10^3 CFU/mL, were cultured in the media or blood. Here, $\Delta C/C_0$, $\Delta G/G_0$, and $\Delta Z/Z_0$ were obtained by subtracting C/C_0, G/G_0, and Z/Z_0 measured in the bacteria-free solution (negative control, Fig. S3) from C/C_0, G/G_0, and Z/Z_0 measured in the *E. coli* solution, respectively, with C_0, G_0, and Z_0 being the initial values. When *E. coli* were cultured in the media, the capacitance and conductance increased, and the impedance decreased over time (blue symbols), as reported previously for a horizontal capacitance sensor (Jo et al., 2018). However, when they were cultured in the blood, the capacitance decreased at $f = 0.5$ kHz (red symbols) and increased at $f = 10$ kHz (magenta symbols). In contrast, the conductance decreased and the impedance increased at both 0.5 and 10 kHz, although they changed very slowly at $f = 10$ kHz, in parallel to the frequency dependences of the capacitance, conductance, and impedance in Fig. 2e – g.

To investigate the role of the aptamers, we also measured the real-time capacitance, conductance, and impedance at $f = 0.5$ kHz using a sensor without aptamers in the blood culture. Compared with the aptasensors, the sensors without aptamers exhibited significantly lower sensitivity, suggesting that the capacitance, conductance, and impedance were more sensitively affected by the *E. coli* bound on the sensor surface via aptamer than by unbound *E. coli*.

An equivalent circuit for blood culture is shown in Fig. 2h. Biofilms formed on both the sensor and electrodes surfaces during the blood culture. Thus, the impedance caused by the biofilm on the sensor surface ($Z_{biofilm\text{-}s}$) was connected with $Z_{solution}$, $Z_{aptamer}$, and $Z_{bacteria}$ in parallel, and the impedance caused by the biofilm on the electrode surface ($Z_{biofilm\text{-}e}$) was connected in series. Therefore, the total impedance (Z_{tot}) was given by

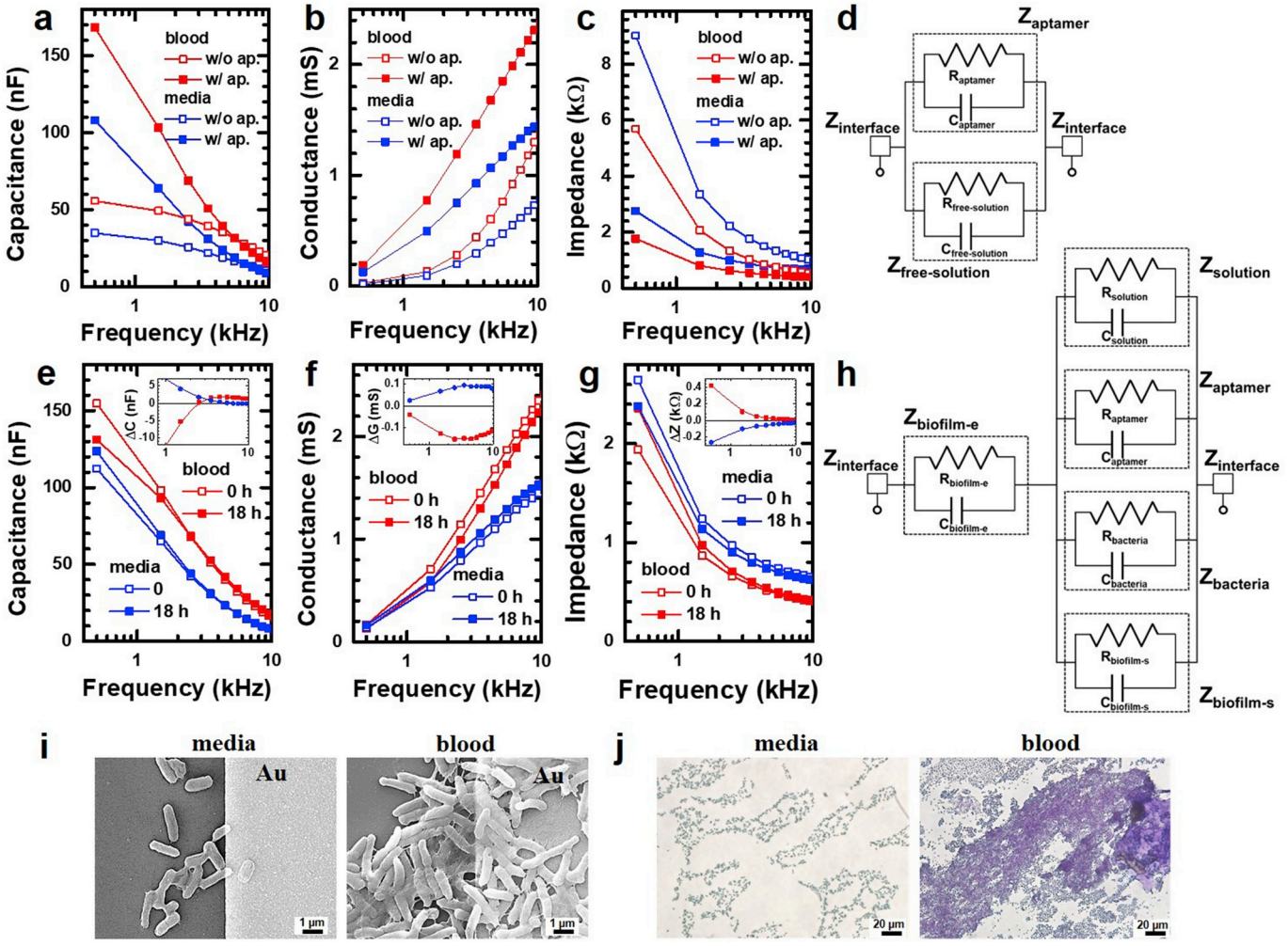

Fig. 2. Analysis of frequency-dependent electrical signals. Frequency dependence of the (**a**) capacitance, (**b**) conductance, and (**c**) impedance in the bacteria-free media and blood before and after the immobilization of the aptamers on the sensor surface. The red and blue symbols indicate the blood and media, respectively; the open and filled symbols represent the data obtained before and after the immobilization of the aptamers, respectively. (**d**) Equivalent circuit for the bacteria-free solution. Frequency dependence of the (**e**) capacitance, (**f**) conductance, and (**g**) impedance for the media and blood cultures. The red and blue symbols indicate the data obtained for the blood and media cultures, respectively; the open and filled symbols represent the data measured at 0 and 18 h after the inoculation of 10^3 CFU/mL *E. coli* into the blood or media. The insets show the capacitance, conductance, and impedance differences measured at 0 and 18 h in the media (blue symbols) and blood (red symbols). The enlarged insets are shown in Fig. S2. (**h**) Equivalent circuit for the blood culture. (**i**) SEM and (**j**) crystal violet stained images of the aptasensors acquired after *E. coli* were cultured for 18 h in the media (left) and blood (right). (For interpretation of the references to color in this figure legend, the reader is referred to the Web version of this article.)

$$Z_{tot} = \left(\frac{1}{Z_{solution}} + \frac{1}{Z_{aptamer}} + \frac{1}{Z_{bacteria}} + \frac{1}{Z_{biofilm-s}} \right)^{-1} + Z_{biofilm-e} \quad (1)$$

where Z_{solution} represents the impedance of the media or blood containing *E. coli*, Z_{aptamer} represents the impedance of the aptamer functionalized on the sensor surface, Z_{bacteria} represents the impedance of the bacteria bound on the sensor surface via the aptamers, $Z_{\text{biofilm-s}}$ represents the impedance of the biofilm on the sensor surface, and $Z_{\text{biofilm-e}}$ represents the impedance of the biofilm on the electrode surface.

Assuming that Z_{bacteria} and Z_{aptamer} were the same for the media and blood cultures and that the contribution of $1/Z_{\text{biofilm-s}}$ was not significant, $Z_{\text{biofilm-e}}$ was estimated at $f = 0.5$ kHz from Fig. 3c and Fig. S3 using Eq. (1), as shown in Fig. 3d. $Z_{\text{biofilm-e}}$ increased over time, and its increasing rate was higher than the decreasing rate of Z_{bacteria} in the media culture (Fig. S4). Accordingly, the increase in $Z_{\text{biofilm-e}}$ caused by the biofilm formation was larger than the decrease in Z_{bacteria} induced by bacterial growth, resulting in an increase in Z_{tot} at $f = 0.5$ kHz in the blood culture. In Fig. 3d, $Z_{\text{biofilm-e}}$ is compared with the area of the biofilm, which was estimated from time-lapse images of the aptasensors stained with crystal violet after *E. coli* of 10^3 CFU/mL were cultured for different growth times. The $Z_{\text{biofilm-e}}$ and the area of the biofilm increased similarly over time, indicating that the biofilm formation increased $Z_{\text{biofilm-e}}$.

In contrast to the electrical properties at $f = 0.5$ kHz, the capacitance at $f = 10$ kHz increased over time, whereas the conductance and impedance at $f = 10$ kHz were nearly unchanged. As shown in Fig. 2g, the impedance decreased with increasing frequency; thus, $Z_{\text{biofilm-e}}$ is expected to be very small at $f = 10$ kHz. In this case, the capacitance increase caused by bacterial growth would be larger than the $Z_{\text{biofilm-e}}$ increase caused by biofilm formation, leading to a capacitance increase at $f = 10$ kHz even in the presence of the biofilm. This is possibly due to the fact that the electric properties were mainly affected by bacterial growth and biofilm formation at $f = 10$ and 0.5 kHz, respectively, because the biofilms were too large to reorient themselves at $f = 10$ kHz, while bacteria much smaller than the biofilm could react to ac fields at $f = 10$ kHz.

To confirm our hypothesis, we prepared two types of *P. aeruginosa*

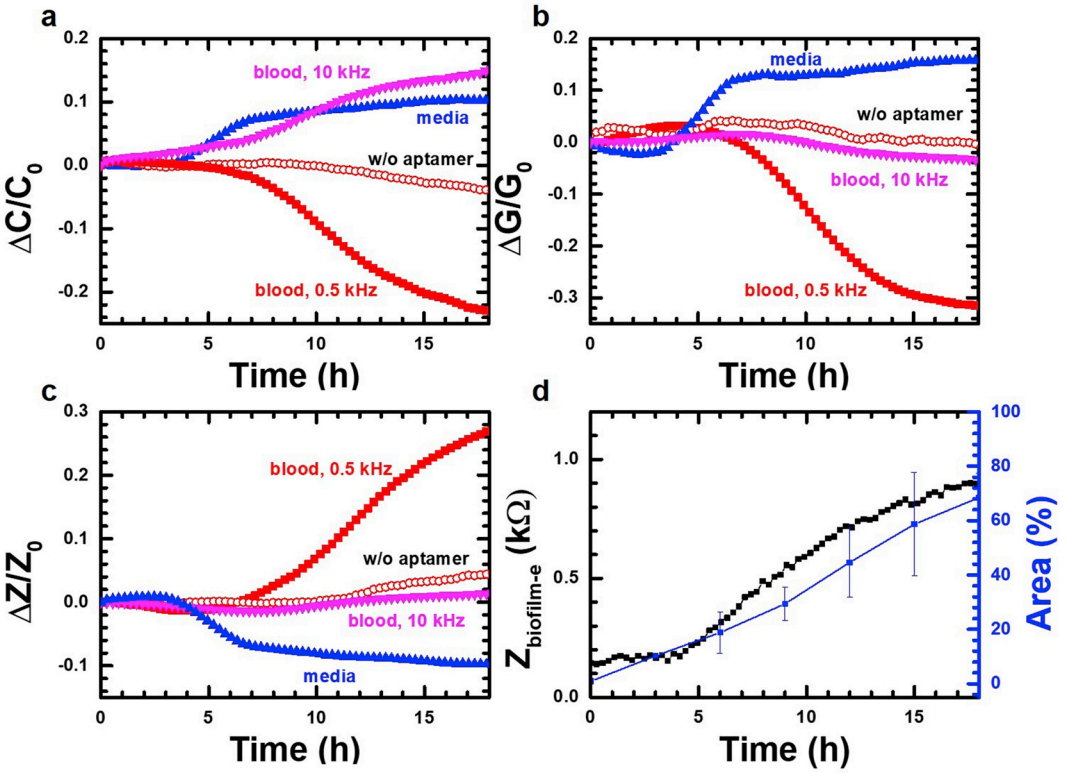

Fig. 3. Real-time electrical properties at different frequencies during bacterial growth. Real-time (**a**) capacitance, (**b**) conductance, and (**c**) impedance measured for the aptasensors at $f = 0.5$ kHz when 10^3 CFU/mL *E. coli* were cultured in the media (blue symbols) and blood (red symbols). The magenta symbols represent the data measured at $f = 10$ kHz for the aptasensor when *E. coli* were cultured in blood, and the open red symbols represent the data measured at $f = 0.5$ kHz for the sensor without aptamers when *E. coli* were cultured in blood. (**d**) $Z_{\text{biofilm-e}}$ estimated using Eq. (1) and the area of the biofilm estimated from time-lapse images of the aptasensors stained with crystal violet. The data are shown as the mean ± standard deviation ($n \geq 3$). (For interpretation of the references to color in this figure legend, the reader is referred to the Web version of this article.)

(PAO1) mutants – *Δpel* (gene *pel* knockout) and *Δpel/Δpsl* (genes *pel* and *psl* knockout) – that hinder biofilm formation, as the *pel* and *psl* genes are important exopolysaccharide elements for surface adherence, intercellular cohesion, and structuring the biofilm (Fig. 4a – c and Fig. S5) (Cooley et al., 2013; Murakami et al., 2017). We measured real-time impedance and capacitance at $f = 0.5$ and 10 kHz when 10^3 CFU/mL wildtype and mutant *P. aeruginosa* were cultured in blood (Fig. 4e – h). The mutant *P. aeruginosa* exhibited a slower increase in impedance and decrease in capacitance at $f = 0.5$ kHz than the wildtype. Furthermore, the *P. aeruginosa* with *Δpel/Δpsl* exhibited slower changes than the *P. aeruginosa* with *Δpel*, which was consistent with the result that biofilm formation was more suppressed for the *P. aeruginosa* with *Δpel/Δpsl* than for the *P. aeruginosa* with *Δpel* (Fig. 4d). We also compared the $Z_{\text{biofilm-e}}$ estimated using Eq. (1) with the biofilm area estimated from the time-lapse images of the aptasensors stained with crystal violet (Fig. S6). Similar increases were observed, indicating that the impedance increase or capacitance decrease at $f = 0.5$ kHz was due to the biofilm formation.

At $f = 10$ kHz, the capacitance increased similarly for the three types of *P. aeruginosa*, despite their different biofilm concentrations (Fig. 4h), confirming that bacterial growth in blood can be monitored in real-time by measuring capacitance change at $f = 10$ kHz. The impedance at $f = 10$ kHz increased more rapidly for the wildtype *P. aeruginosa* than for both mutants; however, these changes were too small to monitor bacterial growth or biofilm formation (Fig. 4f). Hence, we only presented the real-time capacitance measured at $f = 0.5$ and 10 kHz under various conditions.

3.4. Sensitivity of vertical aptasensor

To identify the minimum concentration of bacteria that could be monitored using vertical aptasensors, we measured the real-time capacitance at $f = 10$ and 0.5 kHz when *E. coli* concentrations ranging from 10^0 to 10^3 CFU/mL were cultured in the blood (Fig. 5a and b). At low concentrations, the capacitance was initially unchanged for some time, and then increased at $f = 10$ kHz. As the concentration decreased, the starting point of the capacitance change was delayed, and the capacitance increased more slowly. For 10^0 CFU/mL, the capacitance increased at approximately 12 h, indicating that even 10^0 CFU/mL of *E. coli* in the blood culture media could be detected within 12 h.

Similarly, the capacitance at $f = 0.5$ kHz was initially unchanged. It decreased later and more slowly with the decreasing concentration of *E. coli*. Fig. 5c shows the area of the biofilm estimated from the time-lapse images of the aptasensors stained with crystal violet after different concentrations of *E. coli* were cultured in blood at different times (Fig. S7). As the concentration of *E. coli* decreased, the biofilm formed more slowly. The starting point of the capacitance change was noted to correspond to the time at which the area of the biofilm was approximately 20%. The area of the biofilm was also compared with the $Z_{\text{biofilm-e}}$ estimated using Eq. (1) (Fig. 5c). A strong relationship was observed, confirming that the biofilm formation could be monitored in real-time by measuring capacitance change at $f = 0.5$ kHz.

In addition to *E. coli*, we performed similar measurements with *S. aureus* (Fig. 5d – f and Fig. S8) and *P. aeruginosa* (Figs. S9 and S10), and obtained similar results. This indicates that our vertical sensors can be employed for the real-time monitoring of bacterial growth and biofilm formation in blood for various bacteria at concentrations as low as 10^0 CFU/mL.

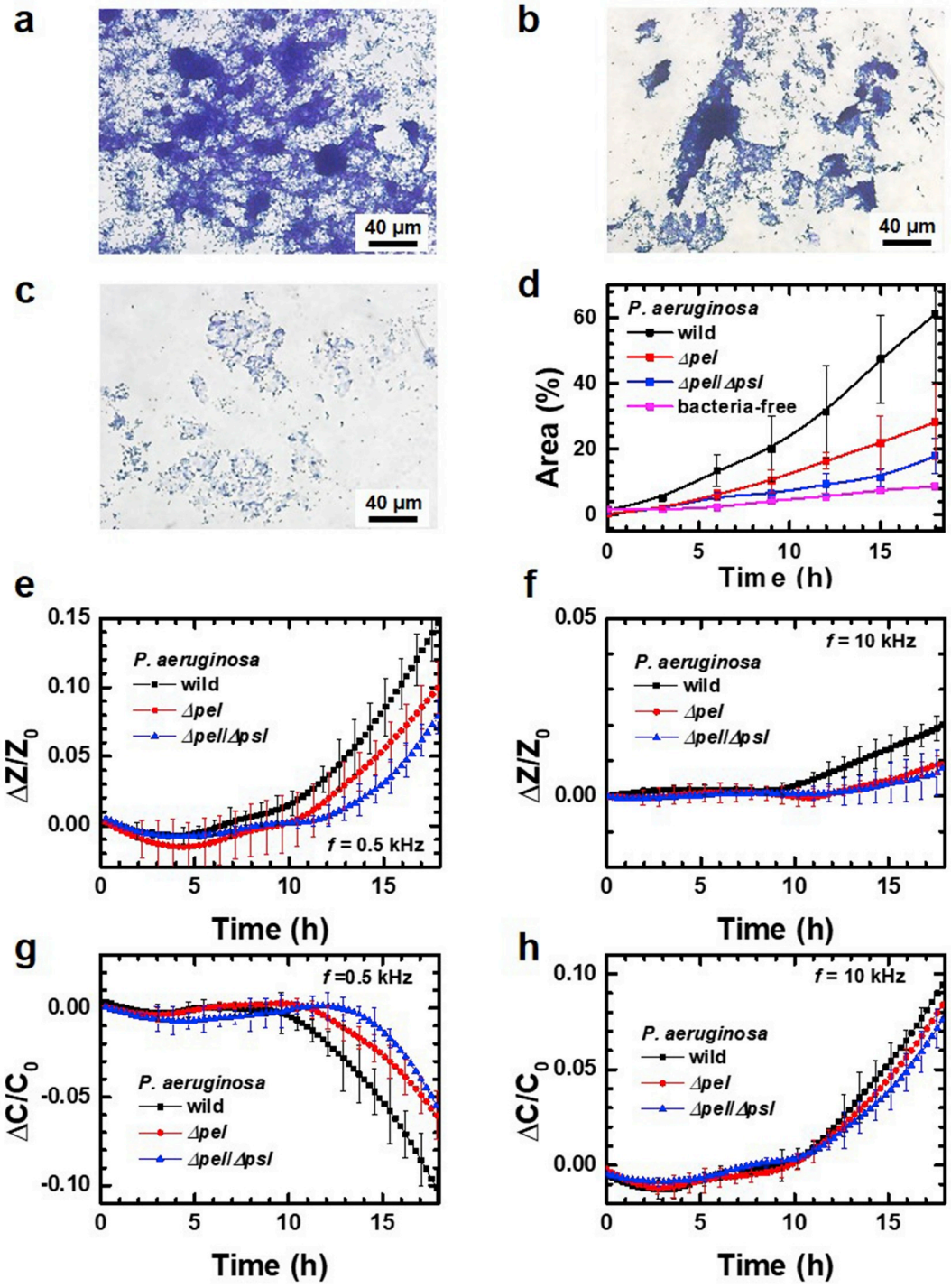

Fig. 4. Influence of biofilm formation on electrical properties for wildtype and mutant-*P. aeruginosa*. Optical images of the aptasensors stained with crystal violet after (**a**) wildtype *P. aeruginosa* PAO1, (**b**) *Δpel* and (**c**) *Δpel/Δpsl* mutant *P. aeruginosa* PAO1 were cultured in blood for 18 h. (**d**) Area of the biofilm estimated from the time-lapse images for wildtype, *Δpel* and *Δpel/Δpsl* mutant *P. aeruginosa* PAO1. Real-time impedance of wildtype and mutants *P. aeruginosa* cultured in blood measured at (**e**) f = 0.5 kHz and (**f**) 10 kHz. Real-time capacitance of the wildtype and mutant *P. aeruginosa* cultured in blood measured at (**g**) f = 0.5 kHz and (**h**) 10 kHz. The data are shown as the mean ± standard deviation ($n \geq 3$).

3.5. Real-time monitoring of antibiotic susceptibility

To investigate whether the vertical aptasensors could also be employed for the AST in blood, we measured the real-time capacitance at $f = 10$ and 0.5 kHz when different concentrations of gentamicin (Fig. 6a and b) or amikacin (Fig. 6d and e) were added to blood containing 10^3 CFU/mL *E. coli*. At $f = 10$ kHz, capacitance increased over time for 0.01 μg/mL gentamicin and ≤0.1 μg/mL amikacin, but remained nearly unchanged for ≥0.1 μg/mL gentamicin and ≥1 μg/mL amikacin. These results indicate that the minimal inhibitory concentration (MIC) for *E. coli* was approximately 0.1 and 1 μg/mL for gentamicin and amikacin, respectively, which is comparable to the values reported by the Clinical Laboratory Standard Institute (CLSI) (Patel et al., 2014). At $f = 0.5$ kHz, the capacitance decreased over time below the MIC, but remained nearly unchanged above the MIC, implying that the biofilm formation was inhibited above the MIC. Indeed,

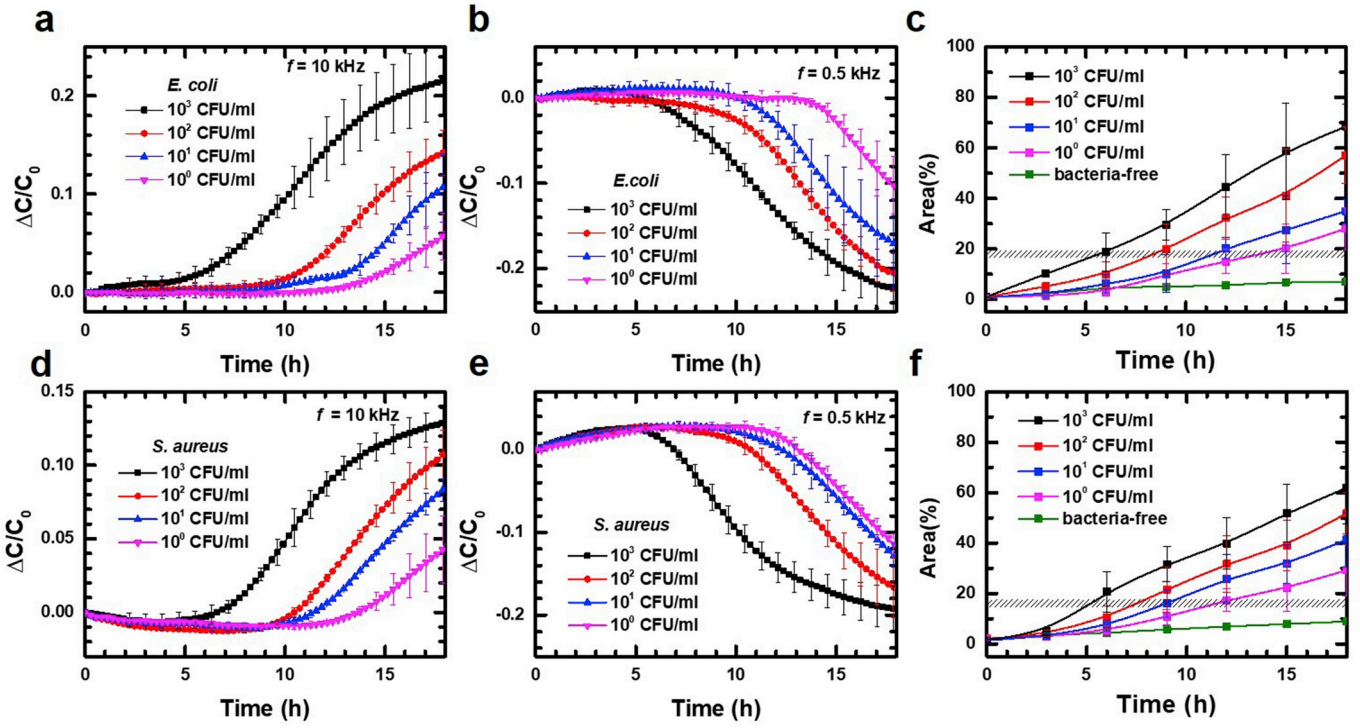

Fig. 5. Real-time monitoring of bacterial growth for *E. coli* and *S. aureus*. Real-time capacitance measured at (**a**) f = 10 kHz and (**b**) 0.5 kHz when different concentrations of *E. coli* were cultured in blood. (**c**) Area of the biofilm estimated from time-lapse images of the aptasensors stained with violet crystal after different concentrations of *E. coli* were cultured in blood for different times. Real-time capacitance measured at (**d**) f = 10 kHz and (**e**) 0.5 kHz when different concentrations of *S. aureus* were cultured in blood. (**f**) Area of the biofilm estimated from time-lapse images of the aptasensors stained with violet crystal after different concentrations of *S. aureus* were cultured in blood for different times. The dashed areas in (**c**) and (**f**) indicate the starting time of the capacitance decrease at f = 0.5 kHz for various concentrations. The data are shown as the mean ± standard deviation ($n \geq 3$).

the biofilm was hardly observed above the MIC (Fig. S11). The area of the biofilm was estimated from the time-lapse images of aptasensors stained with crystal violet after different concentrations of gentamicin or amikacin were added to blood containing 10^3 CFU/mL *E. coli*, followed by culturing at different times (Fig. 6c and f). As expected, the area of the biofilm increased more rapidly with decreasing concentrations of the antibiotic.

Fig. 6g – h shows the real-time capacitance measured at f = 10 and 0.5 kHz, respectively, when 1 μg/mL gentamicin or amikacin solution (0.1 mL) was added 7 h after culturing 10^2 CFU/mL *E. coli* in blood. The capacitance was nearly unchanged to 7 h because the concentration of *E. coli* was low. However, when antibiotic solution or media was added, the capacitance changed; thereafter, the capacitance increased at f = 10 kHz and decreased at f = 0.5 kHz for 0 μg/mL, while the capacitance was nearly unchanged at f = 10 and 0.5 kHz for 1 μg/mL gentamicin and amikacin, which are consistent with the results shown in Fig. 2a – f. We also measured the real-time capacitance at f = 10 kHz when different concentrations of gentamicin in 0.1 mL media were added 15 h after culturing 10^2 CFU/mL *E. coli* in blood (Fig. 6i). The capacitance increased from approximately 10 h after culture, indicating the blood culture positivity. After adding the gentamicin solution, the capacitance at f = 10 kHz remained nearly constant for 100 μg/mL, implying that bacterial growth was inhibited because 100 μg/mL is above the MIC. On the other hand, the capacitance increased for 1 μg/mL because the concentration of *E. coli* was very high owing 15 h culture and bacterial growth was not inhibited by 1 μg/mL gentamicin.

Similar experiments were also performed for *S. aureus* (Fig. S12) and *P. aeruginosa* (Fig. S13). The MIC for *S. aureus* was approximately 1 and 0.1 μg/mL for gentamicin and amikacin, respectively, and that for *P. aeruginosa* was approximately 1 μg/mL for both gentamicin and amikacin. These values are comparable to those reported by the CLSI (Patel et al., 2014), indicating that our vertical aptasensors can also be employed for the real-time monitoring of antibiotic susceptibility in blood.

4. Conclusions

In this study, we developed an aptamer-functionalized sensor (aptasensor) that was vertically connected to a measurement system. When bacteria were cultured in blood (0.2 mL) and culture media (0.8 mL), we found that capacitance changes measured at f = 0.5 and 10 kHz reflected biofilm formation and bacterial growth, respectively, allowing simultaneous monitoring of bacterial growth and biofilm formation. Bacteria (*E. coli*, *S. aureus*, and *P. aeruginosa*) seeded at 10^0–10^3 CFU/mL could be detected within 12 h by measuring capacitance changes at f = 0.5 and 10 kHz, indicating that vertical capacitance aptasensors can be an alternative tool for detecting bacteria in blood. In addition, we investigated whether antibiotic susceptibility in blood could be monitored using the vertical capacitance aptasensor. When bacteria in blood were treated with antibiotics, gentamicin or amikacin below the MIC, the capacitance increased at f = 10 kHz and decreased at f = 0.5 kHz. However, when the concentration of the antibiotic was higher than the MIC, the capacitance remained nearly unchanged at f = 10 and 0.5 kHz, indicating that bacterial growth and biofilm formation were inhibited. These results demonstrate that vertical aptasensor could also be used for rapid ASTs using positive blood cultures without the need for sub-culturing.

Declaration of competing interest

The authors declare that they have no known competing financial interests or personal relationships that could have appeared to influence the work reported in this paper.

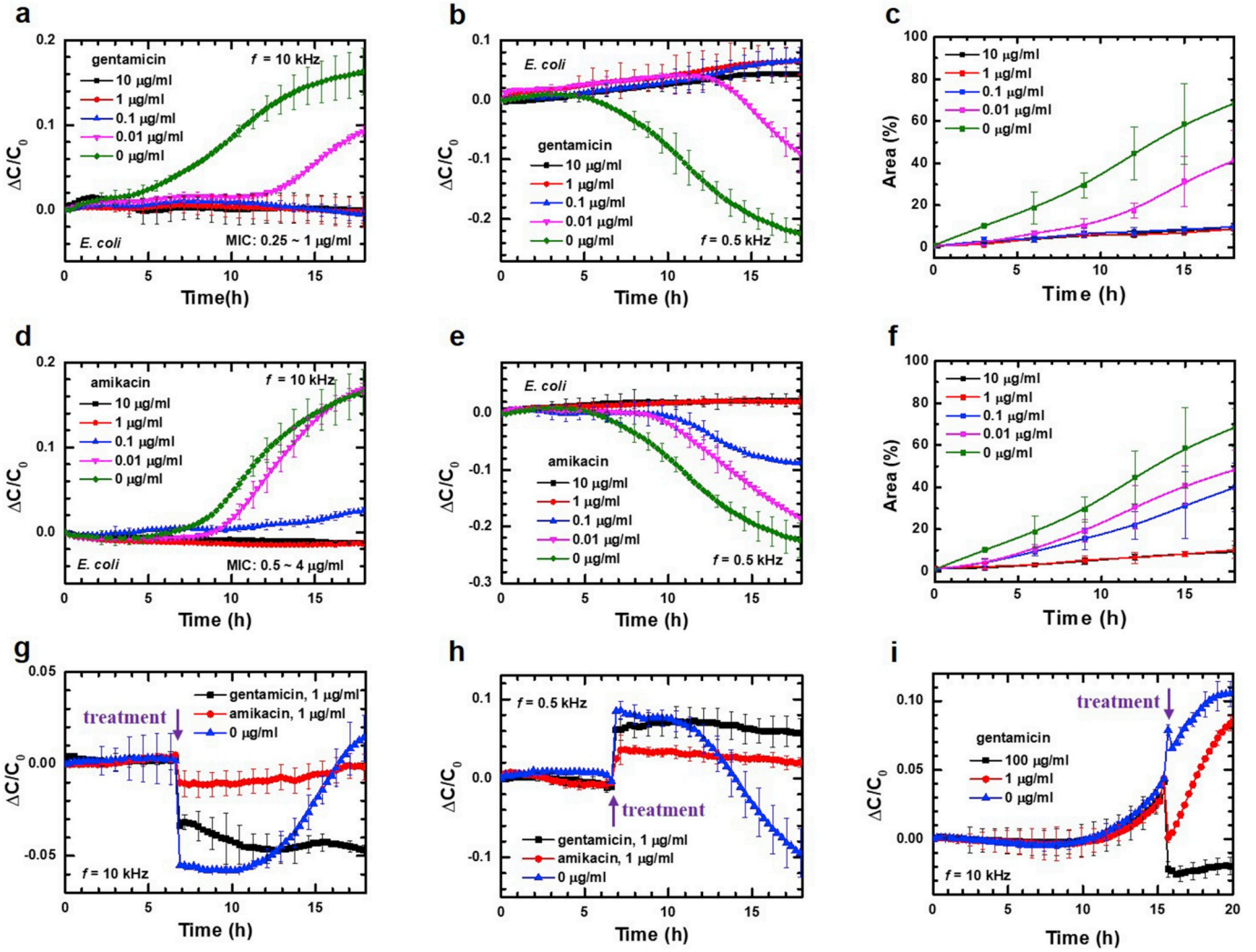

Fig. 6. Real-time monitoring of AST for *E. coli*. Real-time capacitance measured at (**a**) $f = 10$ kHz and (**b**) 0.5 kHz when 10^3 CFU/mL *E. coli* in blood were treated with different concentrations of gentamicin. (**c**) Area of biofilm estimated from time-lapse images of the aptasensors stained with crystal violet after 10^3 CFU/mL *E. coli* in blood were treated with different concentrations of gentamicin for different times. Real-time capacitance measured at (**d**) $f = 10$ kHz and (**e**) 0.5 kHz when 10^3 CFU/mL *E. coli* in blood were treated with different concentrations of amikacin. (**f**) Area of the biofilm estimated from time-lapse images of the aptasensors stained with crystal violet after 10^3 CFU/mL *E. coli* in blood were treated with different concentrations of amikacin for different times. Real-time capacitance measured at (**g**) $f = 10$ kHz and (**h**) 0.5 kHz when 1 μg/mL gentamicin or amikacin solution (0.1 mL) was added 7 h after culturing 10^2 CFU/mL *E. coli* in blood. (**i**) Real-time capacitance measured at $f = 10$ kHz when different concentrations of gentamicin in 0.1 mL media was added 15 h after culturing 10^2 CFU/mL *E. coli* in blood. The real-time capacitance measured at $f = 0.5$ kHz under the same condition is shown in Fig. S14. The data are shown as the mean ± standard deviation ($n \geq 3$).

Acknowledgments

This work was supported by the Nano-Convergence Foundation funded by the Ministry of Science and ICT and the Ministry of Trade, Industry and Energy (Grant no. R201801311), and by Basic Science Research Program through the National Research Foundation of Korea (NRF) funded by the Ministry of Science, ICT and Future Planning (Grant nos. 2016R1A2B3011980, 2016R1A2B4014999, 2019R1H1A2080077, and 2019R1H1A2079842), and NRF funded by the Korean government (MEST) (2017R1A2B3006704 and 2019R1A6A1A03032869) and Brain Korea 21 PLUS Project for Medical Science.

Appendix A. Supplementary data

Supplementary data to this article can be found online at https://doi.org/10.1016/j.bios.2019.111623.

References

Almuhayawi, M., Altun, O., Abdulmajeed, A.D., Ullberg, M., Özenci, V., 2015. PLoS One 10, e0142398.
Balouiri, M., Sadiki, M., Ibnsouda, S.K., 2016. J. Pharm. Anal. 6, 71–79.
Baym, M., Stone, L.K., Kishony, R., 2016. Science 351, aad3292.
Bradley, P., Gordon, N.C., Walker, T.M., Dunn, L., Heys, S., Huang, B., Earle, S., Pankhurst, L.J., Anson, L., de Cesare, M., Piazza, P., Votintseva, A.A., Golubchik, T., Wilson, D.J., Wyllie, D.H., Diel, R., Niemann, S., Feuerriegel, S., Kohl, T.A., Ismail, N., Omar, S.V., Smith, E.G., Buck, D., McVean, G., Walker, A.S., Peto, T.E.A., Crook, D.W., Iqbal, Z., 2015. Nat. Commun. 6, 10063.
Brazelton de Cárdenas, J.N., Su, Y., Rodriguez, A., Hewitt, C., Tang, L., Garner, C.D., Hayden, R.T., 2017. Diagn. Microbiol. Infect. Dis. 89, 52–57.
Caballero-Granado, F.J., Becerril, B., Cuberos, L., Bernabeu, M., Cisneros, J.M., Pacho′n, J., 2001. Clin. Infect. Dis. 32, 587–594.
Chang, J., Park, J.S., Park, S., Choi, B., Yoon, N.S., Sung, H., Kim, M.N., 2015. Diagn. Microbiol. Infect. Dis. 81, 89–93.
Chantell, C., 2015. Clin. Microbiol. Newsl. 37, 161–167.
Cooley, B.J., Thatcher, T.W., Hashmi, S.M., L'Her, G., Le, H.H., Hurwitz, D.A., Provenzano, D., Touhami, A., Gordon, V.D., 2013. Soft Matter 9, 3871–3876.
Jo, N., Kim, B., Lee, S.M., Oh, J., Park, I.H., Lim, K.J., Shin, J.S., Yoo, K.H., 2018. Biosens. Bioelectron. 102, 164–170.
Jorgensen, J.H., Ferraro, M.J., 2009. Clin. Infect. Dis. 49, 1749–1755.

Kim, D.K., Kim, D.M., Yoo, S.M., Lee, S.Y., 2017. RSC Adv. 7, 18815–18820.
Kim, Y.S., Chung, J., Song, M.Y., Jurng, J., Kim, B.C., 2014. Biosens. Bioelectron. 54, 195–198.
Kumar, A., Ellis, P., Arabi, Y., Roberts, D., Light, B., Parrillo, J.E., Dodek, P., Wood, G., Kumar, A., Simon, D., Peters, C., Ahsan, M., Chateau, D., 2009. Chest 136, 1237–1248.
Lancaster, D.P., Friedman, D.F., Chiotos, K., Sullivan, K.V., 2015. J. Clin. Microbiol. 53, 3609–3613.
Leekha, S., Terrell, C.L., Edson, R.S., 2011. Mayo Clin. Proc. 86, 156–167.
Lian, Y., He, F., Wang, H., Tong, F., 2015. Biosens. Bioelectron. 65, 314–319.
Liu, L., Xu, Y., Cui, F., Xia, Y., Chen, L., Mou, X., Lv, J., 2018. Biosens. Bioelectron. 112, 86–92.
Luna, V.A., King, D.S., Gulledge, J., Cannons, A.C., Amuso, P.T., Cattani, J., 2007. J. Antimicrob. Chemother. 60, 555–567.
Murakami, K., Ono, T., Viducic, D., Somiya, Y., Kariyama, R., Hori, K., Amoh, T., Hirota, K., Kumon, H., Parsek, M.R., Miyake, Y., 2017. Antimicrob. Agents Chemother. 61 e02587-16.
Nazemi, E., Hassen, W.M., Frost, E.H., Dubowski, J.J., 2017. Biosens. Bioelectron. 93, 234–240.
Oliveira, D.C., de Lencastre, H., 2002. Antimicrob. Agents Chemother. 46, 2155–2161.
Patel, J.B., Cockerill III, F.R., Alder, J., Bradford, P.A., Eliopoulos, G.M., Hardy, D.J., Hindler, J.A., Jenkins, S.G., Lewis II, J.S., Miller, L.A., Powell, M., Swenson, J.M., Traczewski, M.M., Turnidge, J.D., Weinstein, M.P., Zimmer, B.L., 2014. Performance Standards for Antimicrobial Susceptibility Testing; Twenty-Fourth Informational Supplement, 24th ed. Clinical and Laboratory Standards Institute, Wayne, PA.
Pohlman, J.K., Kirkley, B.A., Easley, K.A., Basille, B.A., Washington, J.A., 1995. J. Clin. Microbiol. 33, 2856–2858.
Pulido, M.R., García-Quintanilla, M., Martín-Peña, R., Cisneros, J.M., McConnell, M.J., 2013. J. Antimicrob. Chemother. 68, 2710–2717.
Safavieh, M., Pandya, H.J., Venkataraman, M., Thirumalaraju, P., Kanakasabapathy, M.K., Singh, A., Prabhakar, D., Chug, M.K., Shafiee, H., 2017. ACS Appl. Mater. Interfaces 9, 12832–12840.
Song, J.H., Lee, S.M., Yoo, K.H., 2018. RSC Adv. 8, 31246–31254.
van Hal, S.J., Jensen, S.O., Vaska, V.L., Espedido, B.A., Paterson, D.L., Gosbell, I.B., 2012. Clin. Microbiol. Rev. 25, 362–386.
Webster, T.A., Sismaet, H.J., Goluch, E.D., 2015. Analyst 140, 7195–7201.
Yilmaz, M., Elaldi, N., Balkan, İ.İ., Arslan, F., Batırel, A.A., Bakıcı, M.Z., Gozel, M.G., Alkan, S., Çelik, A.D., Yetkin, M.A., Bodur, H., Sınırtaş, M., Akalın, H., Altay, F.A., Şencan, İ., Azak, E., Gündeş, S., Ceylan, B., Öztürk, R., Leblebicioglu, H., Vahaboglu, H., Mert, A., 2016. Ann. Clin. Microbiol. Antimicrob. 15, 7.
Zhang, X., Jiang, X., Yang, Q., Wang, X., Zhang, Y., Zhao, J., Qu, K., Zhao, C., 2018. Anal. Chem. 90, 6006–6011.